Editors' Suggestion | Featured in Physics

Estimating Entropy Production from Waiting Time Distributions

Dominic J. Skinner and Jörn Dunkel
Department of Mathematics, Massachusetts Institute of Technology, Cambridge, Massachusetts 02139-4307, USA

(Received 23 May 2021; accepted 17 August 2021; published 1 November 2021)

Living systems operate far from thermal equilibrium by converting the chemical potential of ATP into mechanical work to achieve growth, replication, or locomotion. Given time series observations of intra-, inter-, or multicellular processes, a key challenge is to detect nonequilibrium behavior and quantify the rate of free energy consumption. Obtaining reliable bounds on energy consumption and entropy production directly from experimental data remains difficult in practice, as many degrees of freedom typically are hidden to the observer, so that the accessible coarse-grained dynamics may not obviously violate detailed balance. Here, we introduce a novel method for bounding the entropy production of physical and living systems which uses only the waiting time statistics of hidden Markov processes and, hence, can be directly applied to experimental data. By determining a universal limiting curve, we infer entropy production bounds from experimental data for gene regulatory networks, mammalian behavioral dynamics, and numerous other biological processes. Further considering the asymptotic limit of increasingly precise biological timers, we estimate the necessary entropic cost of heartbeat regulation in humans, dogs, and mice.

DOI: 10.1103/PhysRevLett.127.198101

Living systems break time-reversal symmetry [1,2]. Growth [3], self-replication [2], and locomotion [4] are all irreversible processes, violating the principle of detailed balance, which states that every forward microstate trajectory is as likely to occur as its time-reversed counterpart [1,5–7]. Irreversibility places thermodynamic constraints on sensing [8,9], reproduction [2], and signaling [10] and trade-offs between free energy consumption and the precision, speed, or accuracy of performing some function [8,11]. To quantify these constraints, one has to bound the rate at which free energy is consumed or, equivalently, the entropy production rate (EPR) [5,12,13]. However, most experimental measurements can observe only a small number of degrees of freedom [13–15], making such inference challenging. In particular, many systems are accessible only at the coarsest possible level of two states, such as a gene switching [16] or a molecule docking and undocking to a sensor [9,17]. In these cases, commonly used inference tools cannot be applied, due to the absence of observable coarse-grained currents [18–21] and as the forward and reverse trajectories need not be asymmetric [22–25], even if the underlying system operates far from equilibrium.

Here, we introduce a broadly applicable method that makes it possible to estimate the EPR of a coarse-grained two-state dynamics by measuring the variance of time spent in a state. This is achieved by finding a canonical formulation and then solving a numerical optimization problem to obtain a universal limiting curve, above which the EPRs of all systems with the observed waiting time statistics must lie. We illustrate that this method outperforms a recently introduced thermodynamic uncertainty relation (TUR) [9,18,20,26] on synthetic test data and demonstrate its practical usefulness in applications to experimental data for a gene regulatory network [16], the behavioral dynamics of cows [27], and several other biological processes (Table S1 [28]). Furthermore, by considering a stochastic timer [29–32], we derive an asymptotic formula relating the waiting time variance and the EPR. This analytical result can be used to bound the EPR required to maintain precise biophysical timing processes, which we illustrate on data from experimental measurements [33,34] of heartbeats of humans, dogs, and mice.

We start from the standard assumption [5,35] that mesoscale systems in contact with a heat bath can be described by a Markovian stochastic dynamics on a finite set of discrete states $\{1, \ldots, N_T\}$. Transitions from state i to j occur at rate W_{ij}, so a probability distribution over the states, $p_i(t)$, evolves according to

$$\frac{d}{dt} p_i = \sum_j p_j W_{ji}, \tag{1}$$

with $W_{ii} = -\sum_{j \neq i} W_{ij}$ [5,36]. Assuming that the system is irreducible, meaning there exists a path with nonzero probability between any two states, Eq. (1) has a unique stationary state $\pi = (\pi_i)$, satisfying $0 = \pi W$ and which every initial probability distribution tends to [37]. The EPR at steady state π is [20]

$$\sigma = k_B \sum_{i<j} (\pi_i W_{ij} - \pi_j W_{ji}) \log\left(\frac{\pi_i W_{ij}}{\pi_j W_{ji}}\right), \tag{2}$$

which for isothermal systems, when multiplied by the bath temperature, is the rate of free energy dissipation required to maintain the state away from equilibrium [38]. The system is in thermal equilibrium when the EPR vanishes, which is exactly when detailed balance is satisfied, $\pi_i W_{ij} = \pi_j W_{ji}$, for all i and j.

Only a coarse-grained view of the system is typically available in experiments [24,39], with the observed dynamics taking place on a set of metastates, where a metastate I may contain several underlying states i (Fig. 1). Here, we focus on the common case where only two complementary metastates, A and B, are accessible and the observed trajectory jumps between them (Fig. 1). After observing many such jumps, the distributions $f_A(t)$ and $f_B(t)$ of time spent in A and B can be empirically reconstructed (Fig. 1). As the coarse-grained observations are non-Markovian [40], there may be additional information in conditional statistics [15,39], but these are hard to measure experimentally and we do not consider them here. At first glance, the distributions $f_A(t)$ and $f_B(t)$ alone may not appear to contain much information about the underlying system; however, for an equilibrium system, both $f_A(t)$ and $f_B(t)$ must decay monotonically [41], implying that the schematic example in Fig. 1 reflects an out-of-equilibrium dynamics.

To quantify the extent to which an observed two-state system is out of equilibrium, we reformulate the problem of EPR estimation within an optimization framework, extending the approach introduced in Ref. [39]. Calling the underlying system $\mathcal{S}$, the EPR is $\sigma(\mathcal{S})$, and the observed waiting time distributions are $f_A(t,\mathcal{S})$ and $f_B(t,\mathcal{S})$. If $\mathcal{R}$ describes some other underlying system with the same observables, we cannot know which is the true system. However, we can find a lower bound on the EPR by minimizing over all such $\mathcal{R}$:

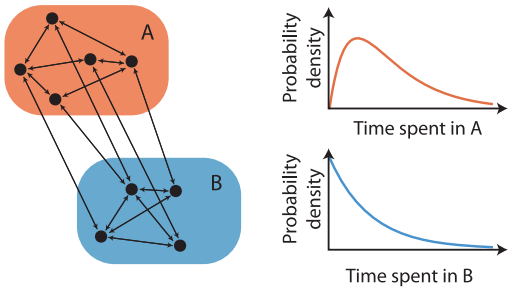

FIG. 1. A Markovian process on discrete states (black circles), observed at a coarse-grained level, with only the metastates A and B visible to the observer (left). From observing this system, we can deduce the distribution of time spent in metastates A and B (right). A nonmonotonic waiting time distribution signals [41] out-of-equilibrium dynamics.

$$\sigma(\mathcal{S}) \geq \min_{\mathcal{R}} \{\sigma(\mathcal{R}) | f_A(t,\mathcal{S}) = f_A(t,\mathcal{R}), \; f_B(t,\mathcal{S}) = f_B(t,\mathcal{R})\}, \tag{3}$$

which holds, since $\mathcal{S}$ is contained in the set on the right. By construction, this is the tightest possible lower bound given the observed distributions f_A and f_B. Limited experimental data may prevent us from precisely measuring the full distribution, but we can typically measure the first few moments $\langle t^n \rangle_A$ and $\langle t^n \rangle_B$. We, therefore, introduce the estimators $\sigma_T^{(n)}$:

$$\sigma(\mathcal{S}) \geq \min_{\mathcal{R}} \{\sigma(\mathcal{R}) | \langle t^k \rangle_{I,\mathcal{R}} = \langle t^k \rangle_{I,\mathcal{S}}, \; \text{for } I = A, B, k = 1, \ldots, n\} \equiv \sigma_T^{(n)}, \tag{4}$$

where $\sigma_T^{(n)} \leq \sigma_T^{(n+1)}$, since increasing n decreases the size of the set over which minimization is performed.

Instead of specifying the transition rates of a system $\mathcal{R}$, we can alternatively specify the net transition rates, $n_{ij} = \pi_i W_{ij}$, for $i \neq j$, provided they satisfy mass conservation at each vertex, $\sum_j n_{ij} = \sum_j n_{ji}$, and independently specify the stationary state π_i. With n_{ij} fixed, modifying π_i does not affect the EPR. In particular, suppose that we have found the optimal π_i, n_{ij}, subject to the constraints; then the fraction of time spent in A is $r_A = \sum_{i \in A} \pi_i$, and similarly $r_B = \sum_{i \in B} \pi_i$. Rescaling $\pi_i \mapsto \pi_i / 2 r_A$ for $i \in A$ and $\pi_i \mapsto \pi_i / 2 r_B$ for $i \in B$ does not affect the EPR but makes the fraction of time spent in each metastate exactly $1/2$. The statistics are rescaled as $\langle t^k \rangle_I \mapsto (1/2 r_I)^k \langle t^k \rangle_I$ for $I = A, B$. The average time spent in A or B in the rescaled system is $\tau = (\langle t \rangle_A + \langle t \rangle_B)/2$. A second rescaling $n_{ij} \mapsto \tau n_{ij}$ with π fixed changes EPR as $\sigma \mapsto \tau \sigma$, and the moments as $\langle t^k \rangle_I \mapsto \langle t^k \rangle_I / \tau^k$. Therefore, we can rewrite Eq. (4) as

$$\sigma(\mathcal{S}) \geq \frac{1}{\tau} \min_{\mathcal{R}} \{\sigma | \langle t^k \rangle_{I,\mathcal{R}} = \langle t^k \rangle_{I,\mathcal{S}} / \langle t \rangle_{I,\mathcal{S}}^k, \; \text{for } I = A, B, k = 2, \ldots, n\}, \tag{5}$$

allowing us to optimize over a single canonical system and rescale to bound any other noncanonical system.

After the canonical rescaling, to express constraints in terms of the transition rates, we label the states so that the first N belong to the metastate A, with $1 \leq N < N_T$, and define $(W_A)_{ij} = W_{ij}$ for $i, j \leq N$, so W_A represents the transitions within A. We also write $\pi = (\pi_A, \pi_B)$, with π_A the first N components of the stationary distribution. For any such Markovian process in the stationary distribution, we have that $f_A(t) = \pi_A W_A^2 \exp(W_A t) \mathbf{1}^T / (-\pi_A W_A \mathbf{1}^T)$ [28,37], and similar for $f_B(t)$. For the canonical system, $\langle t \rangle_{A,\mathcal{R}} = 1$, so $-\pi_A W_A \mathbf{1}^T = 1/2$, and higher moment constraints become

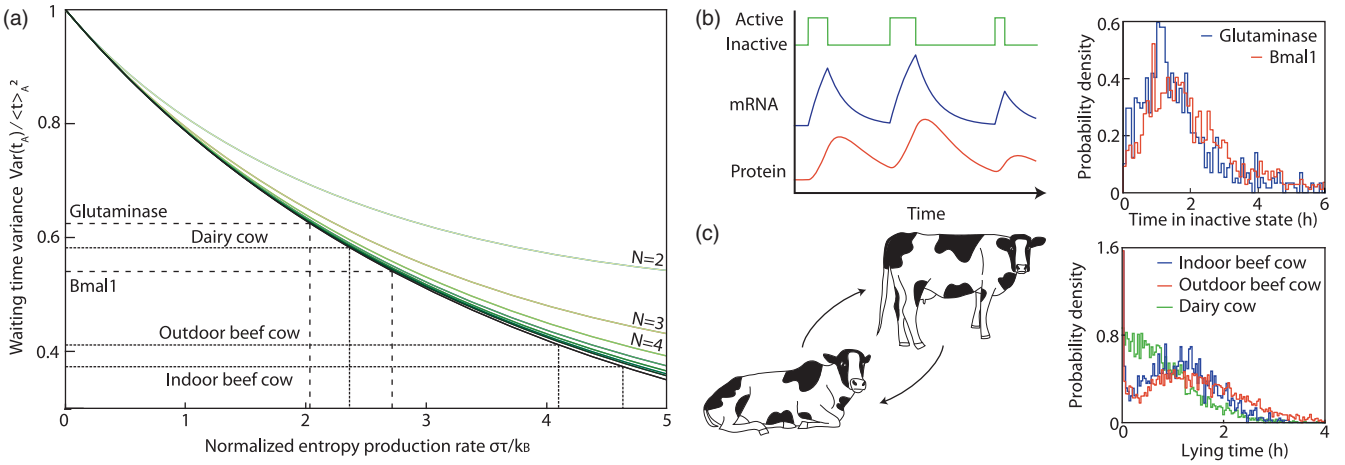

FIG. 2. Bounding the EPR from a single limiting curve. (a) All realizable systems lie above the curve Λ (black) which represents the optimal variance-entropy production trade-off. Minimizing over increasing numbers of internal states leads to rapid convergence, with results shown for up to eight internal states (green curves). Given measured values of the waiting time variance, a lower bound on entropy production can be read off, as demonstrated here for experimental data in (b) (dashed line) and (c) (dotted line). (b) Genes stochastically switch from being active to inactive, mRNA is produced when the gene is active, proteins are produced when mRNA is present, and both stochastically degrade (left). The distribution of time the gene spends in the inactive state as measured in recent experiments, for the genes glutaminase and Bmal1 (right; see also Fig. 2C in Ref. [16]). (c) Distribution of time cows spent lying before standing across three experiments from Ref. [27].

$$\langle t^k \rangle_{A,\mathcal{R}} = 2(-1)^{k+1} k! \pi_A W_A^{1-k} \mathbf{1}^T, \tag{6}$$

and similar for B. While this provides a general minimization framework, from now on we will only impose the constraint on $\langle t^2 \rangle_{A,\mathcal{R}}$, which allows us to minimize over systems with B consisting of a single state [28] and results in a single curve. Specifically, we minimize over $\pi_i > 0$, $n_{ij} \geq 0$, subject to the linear constraints $n_{ii} = -\sum_{j \neq i} n_{ij}$, $\sum_{j \neq i} n_{ij} = \sum_{j \neq i} n_{ji}$, together with $\langle t \rangle_{A,\mathcal{R}} = \langle t \rangle_{B,\mathcal{R}} = 1$, and $\langle t^2 \rangle_{A,\mathcal{R}}$ fixed, finding a curve $k_B \Lambda(\langle t^2 \rangle_{A,\mathcal{R}})$ in the $\sigma - \langle t^2 \rangle_{A,\mathcal{R}}$ plane, or, equivalently, the σ-Var$t_{A,\mathcal{R}}$ plane, above which all Markovian systems must lie [Fig. 2(a)]. For arbitrary systems, this bound becomes

$$\sigma_T = \left[\frac{2k_B}{\langle t \rangle_A + \langle t \rangle_B} \right] \Lambda\left(\frac{\mathrm{Var} t_A}{\langle t \rangle_A^2} \right), \tag{7}$$

which we use throughout to bound the EPR. The function $\Lambda(x)$ can be computed numerically [28,42]; it converges rapidly as the number N of internal states of A is increased [Fig. 2(a)]. Given the tabulated values of Λ, we can apply Eq. (7) directly to experimental data. Before doing so, it is instructive to demonstrate the usefulness of σ_T in simulations of an active sensor.

To perform vital functions like chemotaxis, cells sense chemical concentration levels within their environment [8] through the stochastic binding and unbinding of molecules at surface receptors [9] [Fig. 3(a)]. Recent works [8,9,43] showed that active sensors can overcome the equilibrium Berg-Purcell sensing limit by expending energy, with a trade-off between increased sensing accuracy and energy expended. We apply Eq. (7) to a simple model of an active sensor [9], with the receptor system modeled as a ring with five states, one of which corresponds to an unbound receptor, and with four internal states corresponding to a

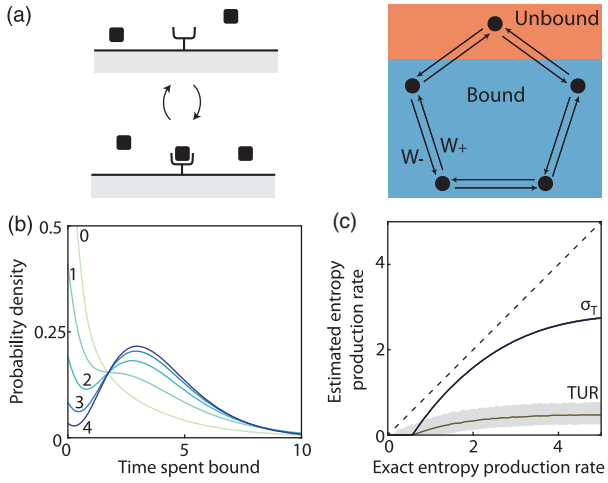

FIG. 3. Bounding the EPR of a model active sensor. (a) Cells sense through receptors on their surface, which detect concentration of some molecular species (black squares) by switching between unbound (top left) and bound (bottom left) configurations. We consider a simple model of a sensor, with four internal states for the bound receptor configuration [9]. Clockwise transitions occur at a rate W_+, and counterclockwise with rate W_-. (b) Distribution of time spent bound for $\sigma = 0, 1, 2, 3, 4$ with $k_B = 1 = W_+, W_- \leq 1$. (c) Estimates of the EPR as a function of the exact EPR σ, as calculated from 200 trajectories of length $T = 2000$ for each value of σ. The σ_T and TUR estimators are shown with 95% range of predictions.

bound receptor [Fig. 3(a)]. The rate of clockwise transitions is taken to be W_+, with counterclockwise transitions occurring at rate $W_- < W_+$, resulting in an EPR of $\sigma = (W_+ - W_-)\log(W_+/W_-)$. The σ_T bound is reasonably close to the exact value σ in intermediate regimes of entropy production [Fig. 3(c)]. For small values of σ, the same variance could be generated by an equilibrium process, whereas for large values the variance could be generated at much lower cost by a system with more internal states [28]. The original TUR [18], while a powerful tool for inference [19,20], cannot gain nontrivial bounds for this system, as there are no observed currents. A more recently introduced TUR [9,28], relating the mean and variance of the fraction of time spent in a metastate to the EPR, is the only existing estimator of which we are aware that can yield a nontrivial bound. Figure 3(c) shows that the TUR bound is substantially lower and for a finite sample size has a much larger variance, thus requiring a large amount of data for a reliable prediction compared to σ_T.

As the first of many experimental applications of σ_T, we consider stochastic gene regulatory networks [44,45]. Cells regulate the intracellular concentration of proteins, changing the concentration in response to external stimuli or maintaining a constant level by balancing production and degradation [45]. Proteins are created by enzymes translating mRNA, which, in turn, is transcribed by enzymes from DNA instructions or genes [46]. Genes switch between active and inactive metastates, the rate of switching regulated by protein concentration, among other things, and while active mRNA is transcribed [44] [Fig. 2(b)]. By examining the distribution of times which a gene spends inactive, we can deduce that the regulatory system is out of equilibrium. Recent experiments [16] on mammalian gene transcription measured the times for which certain genes were active or inactive. From the histogram of inactivity periods [Fig. 2(b)] for the glutaminase gene, one finds $\langle t^2\rangle_{\rm off}/\langle t\rangle^2_{\rm off} = 1.6$ and $\tau = 0.9$ h, so that $\sigma \geq 2.2k_B/\mathrm{h}$, whereas for the Bmal1 promotor, $\langle t^2\rangle_{\rm off}/\langle t\rangle^2_{\rm off} = 1.5$ and $\tau = 1.1$ h, resulting in $\sigma \geq 2.4k_B/\mathrm{h}$.

From complex neural networks to simple feedback loops, living systems make decisions on which behavior to execute, and such decision making requires the expenditure of free energy [47]. Recent experiments identified behavioral states of different organisms [48,49]. From dynamics on these metastates, it is possible to bound the EPR [49]. By attaching sensors to cows, the authors of Ref. [27] recorded whether the cows were standing or lying, as well as the waiting time distribution of each [Fig. 2(c)]. From the time the cows spend lying (metastate A), we can calculate a nonzero bound on the EPR. Specifically, for the three experiments involving pregnant indoor-housed beef cows, out-wintered beef cows, and indoor-housed dairy cows [27], we find $\sigma_T = 4.1k_B/\mathrm{h}$, $3.2k_B/\mathrm{h}$, and $2.4k_B/\mathrm{h}$, respectively. Assuming $k_BT \approx 9.9 \times 10^{-22}$ Cal, we can therefore deduce that the cows consume at least 2.4×10^{-21} Cal/h, in deciding whether to lie or stand. While this is a significant underestimate, the σ_T estimator does not assume any specific model of the decision-making process and so does not require the cows to "possess spherical symmetry" [50].

The systems considered so far could be interpreted as timers; by paying an energetic cost, they control the time spent in a subset of states more precisely than an equilibrium system would allow. Previous studies of biological clocks assume measurements of time are performed by counting the number of full cycles around a circular

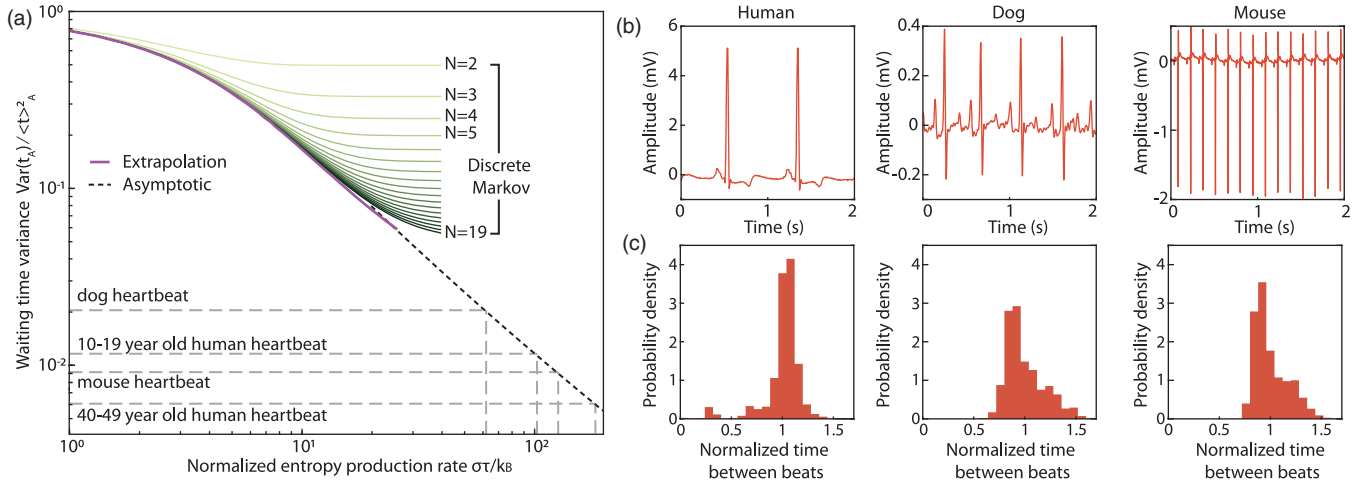

FIG. 4. EPR in the small variance limit. (a) Numerical optimization (green curves) is feasible only for small σ, although extrapolating to $N = \infty$ extends this range (purple line). Alternatively, the asymptotic limit of a continuous Langevin system extends beyond the range of finite networks (dashed line). Using the asymptotic relation, we can examine the entropic cost of building an oscillator as precise as a heartbeat across different species (gray dotted lines). (b) Typical electrocardiogram measurements of heartbeats for humans, dogs, and mice [33,59]. (c) Distribution of time between beats, scaled so the mean time is 1, from a single experiment from each species.

network topology [29], although such analysis can be extended to more general biological oscillators [30,32]. However, the resulting TUR bound cannot be straightforwardly converted into bounds on $\mathrm{Var}t_A$, and, moreover, the networks which saturate the TUR bound do no better than equilibrium systems at minimizing $\mathrm{Var}t_A$ [28]. To elucidate the relationship between σ and $\mathrm{Var}t_A$, one can neglect the dynamics of metastate B by letting $\langle t\rangle_B \to 0$, so that $\sigma \geq (2k_B/\langle t\rangle_A)\Lambda(\mathrm{Var}t_A/\langle t\rangle_A^2)$. Our particular goal is to estimate a bound on the EPR of precise timers exhibiting small variance $\mathrm{Var}t_A/\langle t\rangle_A^2 \ll 1$, such as heartbeats.

Unfortunately, it is not feasible to explore the limit $\mathrm{Var}t_A \to 0$ numerically, as, for a fixed number N of states in A, the largest precision possible is $\mathrm{Var}t_A/\langle t\rangle_A^2 \geq 1/N$, and numerical minimization becomes prohibitively expensive for $N \gtrsim 20$ [28]. To gain analytical insight, we consider the continuum limit of an infinite number of internal states, $N \to \infty$, such that the dynamics in A can be represented by a Langevin equation [28,51]. A continuous system can be approximated arbitrarily well by a discrete system [28,39,52], but a general discrete system need not be well approximated by a continuous Langevin equation [28,53–55], so by searching over the space of Langevin dynamics we will find an upper bound on the true optimal precision versus entropy trade-off curve [28]. In the limit of infinite precision $\mathrm{Var}t_A/\langle t\rangle_A^2 \to 0$, we find analytically [28] the asymptotic relation $\mathrm{Var}t_A/\langle t\rangle_A^2 = 1/\hat{\sigma} + 4\ln\hat{\sigma}/\hat{\sigma}^2 + o(\ln\hat{\sigma}/\hat{\sigma}^2)$, where $\hat{\sigma} = \sigma\langle t\rangle_A/2k_B$; achieving this in practice would require many internal states, a common trade-off in stochastic networks [30,56,57]. We apply this asymptotic prediction to heartbeat data [58] for humans [34] and other species [33]. Although the precision of the observed beating patterns renders numerical σ_T estimates unfeasible, the asymptotic formula implies entropic costs of at least $280k_B/\mathrm{s}$, $480k_B/\mathrm{s}$, $270k_B/\mathrm{s}$, and $2360k_B/\mathrm{s}$ to maintain the heartbeats for young humans, older humans, dogs, and mice, respectively (Fig. 4).

In addition to the systems discussed above, nonequilibrium waiting time distributions have been measured for switching processes in cell fate decision making [60], dwell times of kinesin motors [61,62], cluster lifetimes of RNA polymerase [63], the directional switching of the bacterial motor [41,64], swim-turn dynamics of algae and bacteria [65,66], direction reversal in swarming bacteria [67–69], the repolarization times of migrating cancer cells [70], visual perception switching between metastable states [71], and the duration of animal and insect flights [72,73]. The framework introduced here makes it possible to bound the extent to which these systems are out of equilibrium (Table S1 [28]) and, thereby, to quantify the trade-offs which biological systems are forced to make.

The source code is available online [74].

This work was supported by a MathWorks Fellowship (D. J. S.), a James S. McDonnell Foundation Complex Systems Scholar Award (J. D.), and the Robert E. Collins Distinguished Scholar Fund (J. D.). We thank the MIT SuperCloud and Lincoln Laboratory Supercomputing Center for providing HPC resources.

[1] J. M. R. Parrondo, C. V. den Broeck, and R. Kawai, New J. Phys. **11**, 073008 (2009).
[2] J. L. England, J. Chem. Phys. **139**, 121923 (2013).
[3] P. Wang, L. Robert, J. Pelletier, W. L. Dang, F. Taddei, A. Wright, and S. Jun, Curr. Biol. **20**, 1099 (2010).
[4] J. A. Nirody, Y.-R. Sun, and C.-J. Lo, Adv. Phys. X **2**, 324 (2017).
[5] U. Seifert, Rep. Prog. Phys. **75**, 126001 (2012).
[6] C. Maes, F. Redig, and M. Verschuere, J. Stat. Phys. **106**, 569 (2002).
[7] C. Battle, C. P. Broedersz, N. Fakhri, V. F. Geyer, J. Howard, C. F. Schmidt, and F. C. MacKintosh, Science **352**, 604 (2016).
[8] G. Lan, P. Sartori, S. Neumann, V. Sourjik, and Y. Tu, Nat. Phys. **8**, 422 (2012).
[9] S. E. Harvey, S. Lahiri, and S. Ganguli, arXiv:2002.10567.
[10] K. Thurley, S. C. Tovey, G. Moenke, V. L. Prince, A. Meena, A. P. Thomas, A. Skupin, C. W. Taylor, and M. Falcke, Sci. Signal. (Online) **7**, ra59 (2014).
[11] Y. Cao, H. Wang, Q. Ouyang, and Y. Tu, Nat. Phys. **11**, 772 (2015).
[12] U. Seifert, Phys. Rev. Lett. **95**, 040602 (2005).
[13] U. Seifert, Annu. Rev. Condens. Matter Phys. **10**, 171 (2019).
[14] M. Esposito, Phys. Rev. E **85**, 041125 (2012).
[15] G. Teza and A. L. Stella, Phys. Rev. Lett. **125**, 110601 (2020).
[16] D. M. Suter, N. Molina, D. Gatfield, K. Schneider, U. Schibler, and F. Naef, Science **332**, 472 (2011).
[17] M. Skoge, S. Naqvi, Y. Meir, and N. S. Wingreen, Phys. Rev. Lett. **110**, 248102 (2013).
[18] T. R. Gingrich, J. M. Horowitz, N. Perunov, and J. L. England, Phys. Rev. Lett. **116**, 120601 (2016).
[19] J. Li, J. M. Horowitz, T. R. Gingrich, and N. Fakhri, Nat. Commun. **10**, 1666 (2019).
[20] J. M. Horowitz and T. R. Gingrich, Nat. Phys. **16**, 15 (2020).
[21] M. Polettini and M. Esposito, Phys. Rev. Lett. **119**, 240601 (2017).
[22] F. S. Gnesotto, G. Gradziuk, P. Ronceray, and C. P. Broedersz, Nat. Commun. **11**, 5378 (2020).
[23] E. Roldán and J. M. R. Parrondo, Phys. Rev. Lett. **105**, 150607 (2010).
[24] I. A. Martínez, G. Bisker, J. M. Horowitz, and J. M. R. Parrondo, Nat. Commun. **10**, 3542 (2019).
[25] É. Roldán, J. Barral, P. Martin, J. M. R. Parrondo, and F. Jülicher, arXiv:1803.04743.
[26] T. Van Vu, V. T. Vo, and Y. Hasegawa, Phys. Rev. E **101**, 042138 (2020).
[27] B. J. Tolkamp, M. J. Haskell, F. M. Langford, D. J. Roberts, and C. A. Morgan, Applied animal behaviour science **124**, 1 (2010).

[28] See Supplemental Material at http://link.aps.org/supplemental/10.1103/PhysRevLett.127.198101 for details of analytical and numerical calculations.
[29] A. C. Barato and U. Seifert, Phys. Rev. X **6**, 041053 (2016).
[30] R. Marsland, W. Cui, and J. M. Horowitz, J. R. Soc. Interface **16**, 20190098 (2019).
[31] A. N. Pearson, Y. Guryanova, P. Erker, E. A. Laird, G. A. D. Briggs, M. Huber, and N. Ares, Phys. Rev. X **11**, 021029 (2021).
[32] C. del Junco and S. Vaikuntanathan, J. Chem. Phys. **152**, 055101 (2020).
[33] J. A. Behar, A. A. Rosenberg, I. Weiser-Bitoun, O. Shemla, A. Alexandrovich, E. Konyukhov, and Y. Yaniv, Frontiers of oral physiology **9**, 1390 (2018).
[34] K. Umetani, D. H. Singer, R. McCraty, and M. Atkinson, J. Am. Coll. Cardiol. **31**, 593 (1998).
[35] M. Esposito and C. Van den Broeck, Phys. Rev. E **82**, 011143 (2010).
[36] N. G. Van Kampen, *Stochastic Processes in Physics and Chemistry* (Elsevier, New York, 1992), Vol. 1.
[37] G. Rubino and B. Sericola, J. Appl. Probab. **26**, 744 (1989).
[38] H. Ge and H. Qian, Phys. Rev. E **87**, 062125 (2013).
[39] D. J. Skinner and J. Dunkel, Proc. Natl. Acad. Sci. U.S.A. **118**, e2024300118 (2021).
[40] A. M. Jurgens and J. P. Crutchfield, J. Stat. Phys. **183**, 32 (2021).
[41] Y. Tu, Proc. Natl. Acad. Sci. U.S.A. **105**, 11737 (2008).
[42] Z. Ugray, L. Lasdon, J. Plummer, F. Glover, J. Kelly, and R. Martí, INFORMS J. Comput. **19**, 328 (2007).
[43] A. H. Lang, C. K. Fisher, T. Mora, and P. Mehta, Phys. Rev. Lett. **113**, 148103 (2014).
[44] C. Jia, P. Xie, M. Chen, and M. Q. Zhang, Sci. Rep. **7**, 16037 (2017).
[45] P. C. Bressloff, J. Phys. A **50**, 133001 (2017).
[46] J. Paulsson, Phys. Life Rev. **2**, 157 (2005).
[47] P. Mehta and D. J. Schwab, Proc. Natl. Acad. Sci. U.S.A. **109**, 17978 (2012).
[48] N. Cermak, S. K. Yu, R. Clark, Y.-C. Huang, S. N. Baskoylu, and S. W. Flavell, eLife **9**, e57093 (2020).
[49] K. Y. Wan and R. E. Goldstein, Phys. Rev. Lett. **121**, 058103 (2018).
[50] S. D. Stellman, Science **182**, 1296 (1973).
[51] G. A. Pavliotis, *Stochastic Processes and Applications* (Springer, New York, 2014), Vol. 60.
[52] V. Y. Chernyak, M. Chertkov, and C. Jarzynski, J. Stat. Mech. (2006) P08001.
[53] D. M. Busiello, J. Hidalgo, and A. Maritan, New J. Phys. **21**, 073004 (2019).
[54] T. Herpich, K. Shayanfard, and M. Esposito, Phys. Rev. E **101**, 022116 (2020).
[55] J. M. Horowitz, J. Chem. Phys. **143**, 044111 (2015).
[56] I. Lestas, G. Vinnicombe, and J. Paulsson, Nature (London) **467**, 174 (2010).
[57] J. Yan, A. Hilfinger, G. Vinnicombe, and J. Paulsson, Phys. Rev. Lett. **123**, 108101 (2019).
[58] M. Costa, A. L. Goldberger, and C.-K. Peng, Phys. Rev. Lett. **95**, 198102 (2005).
[59] A. L. Goldberger, L. A. N. Amaral, L. Glass, J. M. Hausdorff, P. C. Ivanov, R. G. Mark, J. E. Mietus, G. B. Moody, C.-K. Peng, and H. E. Stanley, Circulation **101**, e215 (2000).
[60] T. M. Norman, N. D. Lord, J. Paulsson, and R. Losick, Nature (London) **503**, 481 (2013).
[61] H. Isojima, R. Iino, Y. Niitani, H. Noji, and M. Tomishige, Nat. Chem. Biol. **12**, 290 (2016).
[62] C. L. Asbury, A. N. Fehr, and S. M. Block, Science **302**, 2130 (2003).
[63] I. I. Cisse, I. Izeddin, S. Z. Causse, L. Boudarene, A. Senecal, L. Muresan, C. Dugast-Darzacq, B. Hajj, M. Dahan, and X. Darzacq, Science **341**, 664 (2013).
[64] F. Bai, R. W. Branch, D. V. Nicolau, T. Pilizota, B. C. Steel, P. K. Maini, and R. M. Berry, Science **327**, 685 (2010).
[65] M. Theves, J. Taktikos, V. Zaburdaev, H. Stark, and C. Beta, Biophys. J. **105**, 1915 (2013).
[66] M. Polin, I. Tuval, K. Drescher, J. P. Gollub, and R. E. Goldstein, Science **325**, 487 (2009).
[67] Y. Wu, A. D. Kaiser, Y. Jiang, and M. S. Alber, Proc. Natl. Acad. Sci. U.S.A. **106**, 1222 (2009).
[68] O. Sliusarenko, J. Neu, D. R. Zusman, and G. Oster, Proc. Natl. Acad. Sci. U.S.A. **103**, 1534 (2006).
[69] A. Be'er, S. K. Strain, R. A. Hernández, E. Ben-Jacob, and E.-L. Florin, J. Bacteriol. **195**, 2709 (2013).
[70] F. Zhou, S. A. Schaffer, C. Schreiber, F. J. Segerer, A. Goychuk, E. Frey, and J. O. Rädler, PLoS One **15**, e0230679 (2020).
[71] K. Krug, E. Brunskill, A. Scarna, G. M. Goodwin, and A. J. Parker, Proc. R. Soc. B **275**, 1839 (2008).
[72] K. H. Elliott, R. D. Bull, A. J. Gaston, and G. K. Davoren, Behav. Ecol. Sociobiol. **63**, 1773 (2009).
[73] N. E. Raine and L. Chittka, Entomol. Gen. **29**, 179 (2007).
[74] https://github.com/Dom-Skinner/EntropyProductionFromWaitingTimes.